Rev.Adv.Mater.Sci. 4 (2003) 15-24

ELECTRICAL BEHAVIOR OF SEMICONDUCTING NANOPOWDERS VERSUS ENVIRONMENT

Marie-Isabelle Baraton[1] and Lhadi Merhari[2]

[1]SPCTS – UMR 6638 CNRS, Faculty of Sciences, 123 Avenue Albert Thomas, F-87060 Limoges, France
[2]CERAMEC R&D, 64, Avenue de la Libération, F-87000 Limoges, France

Received: February 19, 2003

Abstract. When applied to the study of semiconducting nanosized particles, Fourier transform infrared spectroscopy allows the simultaneous analysis of the chemical reactions occurring at the nanoparticle surface and the resultant variations of the electrical conductivity. This technique has been used to compare the sensing potentiality of three semiconductors (tin oxide, indium oxide and tungsten oxide nanoparticles) before they are integrated in the fabrication process of actual gas sensors.
It has been found that the sensitivity to CO of tin oxide and indium oxide nanoparticles is fairly good, whereas that of tungsten oxide is quasi nil. However, tungsten oxide, like indium oxide, is very sensitive to oxygen and reducing treatments. The presence of humidity irreversibly affects the response of tin oxide to CO and oxygen, whereas that of indium and tungsten oxides to both gases seems to be relatively independent from the moisture content. It is generally observed that a higher operating temperature leads to a more stable baseline and a faster response. Moreover, the formation of surface carbonate groups observed in several cases under CO adsorption does not imply a larger response, thus confirming that the carbonate formation is not a significant factor in the CO detection mechanism.

1. INTRODUCTION

The growing concern worldwide about the consequences of urban air pollution on public health has generated an increasing demand for outdoor air quality monitoring. The European Union, for example, has established directives setting the maximum acceptable concentrations of pollutant gases at very low levels which should steadily be reached in the forthcoming years [1]. Therefore, the market for cost-effective gas sensors capable of detecting pollutants at sub-ppm levels is rapidly growing. Sensitivity, selectivity and obviously reliability are the necessary properties which should be optimized at best while keeping device fabrication at low cost. Semiconductor-based gas sensors fabricated by screen-printing technology meet the latter requirement, that is cost-effectiveness. However, although widely commercialized for indoor air quality monitoring, their performances need to be increased for outdoor air quality monitoring.

In previous works, we have demonstrated that the use of semiconducting nanosized particles in the fabrication of these thick-film gas sensors drastically enhances their sensitivity [2-5]. By using nanoparticles, the detection limits can indeed be decreased below the threshold concentration values set by the international organizations in charge of environment protection.

However, improvements have still to be made, particularly regarding the reproducibility of the chemical composition of the nanoparticle surface. This is a critical parameter controlling the reproducibility of the gas sensor performances. The detection limits can also be strongly influenced by surface contaminants poisoning adsorption sites. Therefore, a perfect control of the nanoparticles surface and a good knowledge of the chemistry at the gas-solid interface

Corresponding author: Marie-Isabelle Baraton, e-mail: baraton@unilim.fr

become requirements for further optimization of semiconductor gas sensors.

2. THEORETICAL BACKGROUND

2.1. Semiconducting nanoparticles

When the size of a particle reaches the nanometer scale, the particle itself can be considered as a surface in three dimensions [6]. As a consequence, the surface reactivity of the nanoparticle is increased due to the increase of the specific surface area, and the interface between the nanoparticle and its surrounding media plays a major role compared to the bulk. In addition, the strong curvature of the surface due to the small radius of the nanoparticle leads to an increased density of the defect sites at the nanoparticle surface. These defect sites are usually strongly reactive and enhance the overall surface reactivity of the nanoparticle compared to its micron-sized counterpart.

Besides, in semiconducting nanoparticles, the Debye length may be comparable to the radius of the particle, which is of importance for electrical properties [7]**.** Indeed, when the particle diameter is much larger than twice the Debye length, the conductance is controlled by the grain boundary. When the particle size is decreased, the necks are the factors controlling the conductance. But when the particle diameter becomes comparable to the Debye length, then the conductance is controlled by the grain, that is by the nanoparticle itself. Therefore, depending on the environment, the thickness of the depletion layer can vary from nearly zero to the entire nanoparticle size and the electrical conductance will be modulated in the entire nanoparticle by the variations of the environment composition. This is an obvious asset for improving the sensitivity of the gas sensor.

2.2. Fundamentals of the gas detection mechanism

It is well-known that the gas detection by chemical sensors based on semiconducting materials is due to electrical conductivity variations induced by adsorption of gases on the semiconductor surface [8].

For example, when oxygen adsorbs on a semiconductor, negatively charged oxygen species (or ionosorbed species) are formed [8,9]:

$$O_2 + 2e^- \rightarrow 2\ O^-_{ads}\ ,$$

$$O_2 + e^- \rightarrow O^-_{2\ ads}\ .$$

The oxygen ionosorption causes electron transfer from the surface of the grain toward the adsorbed species, thus leading to the formation of an electron-depleted surface layer. As a result, the electrical conductivity of a n-type semiconductor decreases.

On the contrary, when a reducing gas, such as CO, adsorbs, electrons are injected into the conduction band and the electrical conductivity of a n-type semiconductor increases. When CO adsorbs in presence of ionosorbed oxygen, the following reactions can possibly occur [10, 11]:

$$2CO + O^-_{2\ ads} \rightarrow 2CO_2 + e^-\ ,$$

$$CO + O^-_{ads} \rightarrow CO_2 + e^-\ ,$$

$$CO + 2O^-_{ads} \rightarrow CO^{2-}_{3\ ads}\ .$$

The first two reactions which produce delocalized electrons are responsible for electrical conductivity changes.

2.3. FTIR absorption and electrical conductivity

The analysis of nanosized particles by Fourier transform infrared (FTIR) transmission spectroscopy brings information on the bulk, surface and space charge simultaneously [12-14]. When free carriers are present in the material (conductor or semiconductor), they also contribute to the background absorption in the infrared range. A variation of the free carrier density, leading to a variation of the thickness of the depletion layer or, in other words, to a variation of the electrical conductivity, translates into a variation of the infrared background absorption [15-18]. Therefore, a thorough analysis of the infrared spectrum theoretically allows one to obtain information on:

- the interatomic bonds constituting the bulk
- the chemical nature of the surface bonds and surface groups
- the possible presence of contaminating species on the surface
- the nature of the adsorption sites
- the free carrier density, in the case of a semiconductor
- the surface reactions and interactions in presence of whatever gaseous environment.

Particularly, when this technique is applied to nanoparticles, the contribution of the surface to the infrared absorption spectrum is no longer negligible due to the high surface-to-bulk ratio.

The variations of the background infrared absorption can therefore be related to the variations of the electrical conductivity. So, in other words, an increase of the electrical conductivity leads to a

decrease of the transmitted infrared energy whereas a decrease of the electrical conductivity leads to an increase of the transmitted infrared energy.

Therefore, the FTIR technique makes it possible to correlate the surface reactions with the changes of the electrical conductivity induced by the surface reactions. This correlation is precisely the underlying mechanism of gas detection by semiconducting materials. It must be emphasized that FTIR spectroscopy allows one to monitor these variations of the electrical conductivity versus gaseous environment on the nanoparticles themselves, thus making it possible to screen the gas sensing potentiality of a nanopowder before embarking in the actual fabrication the gas sensor.

3. EXPERIMENTAL PROCEDURE

In this study, three n-type semiconductor nanopowders, namely tin, indium and tungsten oxides, with a similar average grain size (around 15 nm) have been compared.

As previously mentioned, the FTIR experiments allow one to characterize the surface chemical composition and to simultaneously study the surface reactions and the resulting electrical conductivity variations when the atmosphere is changing around the semiconductor.

The experimental details have already been described elsewhere [12, 19]. To briefly summarize, the nanopowder is slightly pressed into a thin pellet which simulates the gas sensor, during the FTIR surface analyses. The pellet is pre-treated by heating under vacuum to clear the nanoparticle surface from contaminating species and then, the pellet undergoes an oxidizing treatment under pure oxygen to ensure the surface reproducibility over different batches. To screen the gas sensing properties of the nanopowders, the pellets are subjected to oxygen and carbon monoxide at either 300 °C or 150 °C because the real sensors fabricated from these nanopowders have been proved to have CO sensitivity maxima around these temperatures [2, 4]. Surface reactions are analysed *in situ*. The variations of the total infrared energy transmitted by the nanopowder pellet are measured during “oxygen addition/carbon monoxide addition/evacuation” sequences. Simultaneously, the infrared spectrum of the sample is recorded at each step of the experiment to follow the evolution of the surface reactions.

It must be kept in mind that the results of any surface analysis depend on many parameters including the experimental procedure for the surface characterization. Therefore, the chemical composition of a material surface is not an intrinsic characteristics. This is particularly critical for nanosized particles. One of the important consequences is that the composition of the grain boundaries in a sintered nanopowder depends on the synthesis history of the material and on the environmental conditions under which the nanopowder was stored and handled before and during sintering. Moreover, the sensing properties which essentially depend on the reactions at the gas-solid interface are strongly related to the surface reactivity and influenced by the adsorbed chemical species. Therefore, it is of critical importance to define a systematic approach for surface characterization and subsequent follow up of the chemical reactions at the gas-solid interface. It must also be clear that all the results which involve surfaces are obtained for a specific set of parameters and may no longer be valid under different conditions. This makes comparison between differently synthesized or differently processed samples extremely difficult, perhaps even meaningless.

4. RESULTS AND DISCUSSION

4.1. Tin oxide nanoparticles

Fig. 1a shows the spectrum of the tin oxide nanopowder recorded at 300 °C under 50 mbar of oxygen, that is corresponding to fully oxidized tin oxide. The main chemical species present on the surface of the tin oxide nanoparticles are hydroxyl groups either isolated or hydrogen-bonded. All these OH groups absorb in the highest wavenumber region of the spectrum. When CO is adsorbed in presence of oxygen (Fig. 1b), an increase of the background absorption is immediately noted. As previously explained, this change in the background absorption corresponds to the expected increase of the electrical conductivity under this reducing gas. In addition, new infrared absorption bands appear at 1420 and 1375 cm^{-1} and are respectively assigned to newly formed carbon dioxide and surface carbonate species [20-23]. Both carbon dioxide and carbonate species are totally eliminated by evacuation (Fig. 1c).

The electrical conductivity increase is due to the additional delocalized electrons generated by the oxidation reaction of CO into CO_2 as explained in the previous section. Additionally, part of the newly formed carbon dioxide adsorbs on the O^{2-} basic surface sites to form carbonate groups according to this reaction [22]:

$$CO_2 + O_s^{2-} \rightarrow CO_{3\,ads}^{2-}.$$

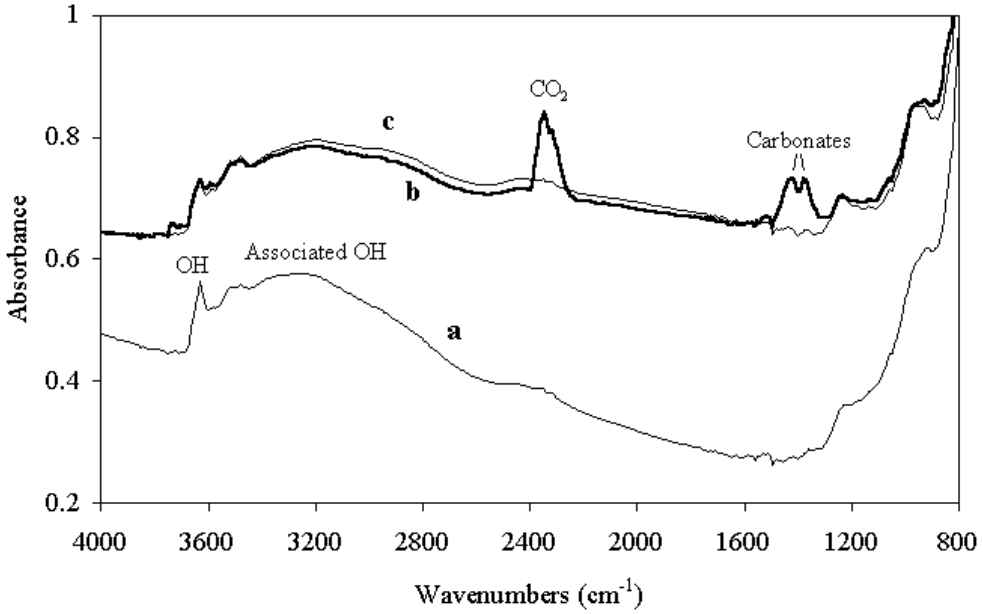

Fig. 1. Infrared transmission spectrum of the SnO_2 nanoparticles at 300 °C: a) under 50 mbar oxygen; b) after adsorption of 10 mbar CO in presence of oxygen; c) after evacuation.

Indeed, additional experiments [5] have proven that carbon dioxide is first formed and it then reacts with the basic surface sites leading to reversible surface carbonates but without any change of the electrical conductivity.

In Fig. 2a are reported the variations of the infrared energy (E_{IR}) transmitted by the tin oxide nanoparticles versus gas exposures at 300 °C. An increase of the transmitted infrared energy corresponds to a decrease of the overall IR absorption, that is to a decrease of the electrical conductivity. At the beginning of the experiment, the sample is under vacuum, that is in a reduced state. When oxygen is in contact with the sample, the transmitted infrared energy rapidly increases, indicating a decrease of the electrical conductivity. The electrical conductivity decrease results from the decrease of the density of free electrons caused by the removal of the oxygen vacancies which were created by the thermal desorption. Then, carbon monoxide

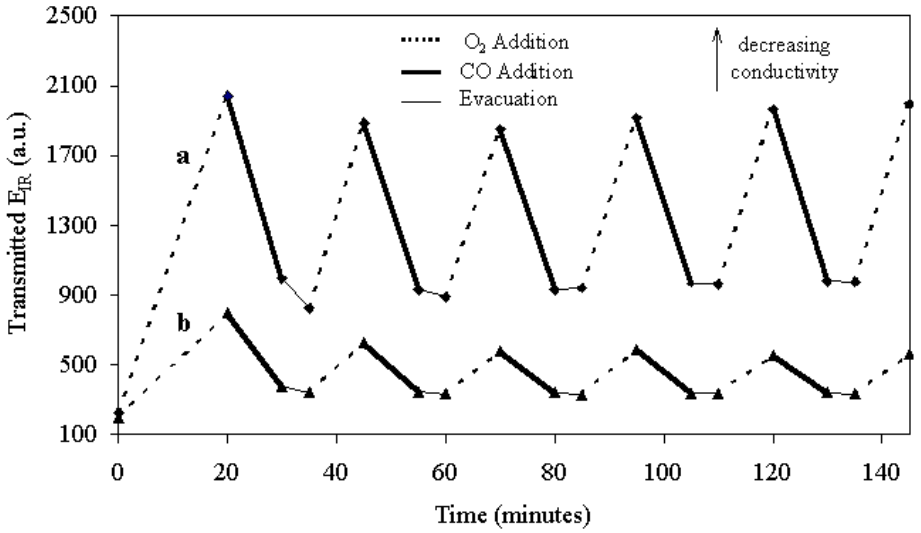

Fig. 2. Variations of the infrared energy (E_{IR}) transmitted by the SnO_2 nanoparticles versus gas exposures: a) at 300 °C; b) at 150 °C.

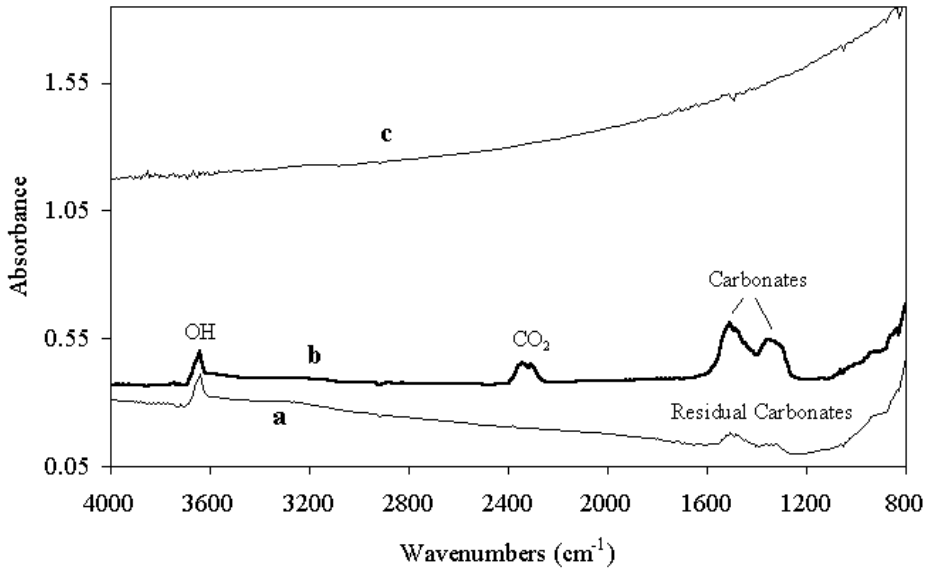

Fig. 3. Infrared transmission spectrum of the In_2O_3 nanoparticles at 300 °C: a) under 50 mbar oxygen; b) after adsorption of 10 mbar CO in presence of oxygen; c) after evacuation.

is adsorbed in presence of oxygen. The transmitted infrared energy decreases showing an increase of the electrical conductivity originating from the carbon dioxide formation which releases free electrons in the conduction band. A quick evacuation followed by an addition of a new dose of oxygen leads to a recovery of the oxidation state and quite reproducible variations of the infrared energy are observed during the "CO addition-evacuation-oxygen addition" sequences.

The same experiment was performed at 150 °C (Fig. 2b). At this lower temperature, the oxidation under oxygen is not complete. Each CO addition leads to a sample reduction via CO_2 formation but surface carbonates are not detected on the infrared spectra (not shown). The subsequent additions of oxygen do not totally restore the oxidation state and each "CO addition-evacuation-oxygen addition" sequence causes a steady overall reduction of the tin oxide powder.

It must be stressed that these curves can be directly compared to the sensor response curves and all these results have been confirmed by electrical measurements performed on the real sensors [2, 4]. However, the lapse of 10 minutes between two measurements has been chosen to make sure that the system has reached the chemical equilibrium and that the surface reactions are completed. It does not correspond to the response time of the real sensor which actually is less than 30 seconds [4].

4.2. Indium oxide nanoparticles

Similar experiments were performed on indium oxide. The infrared spectrum of the indium oxide nanoparticles recorded at 300 °C under oxygen is presented in Fig. 3a. Like in the case of tin oxide, the band in the highest wavenumber region corresponds to surface hydroxyl groups. But in addition, the bands between 1600 and 1200 cm^{-1} indicate the presence of residual carbonate groups on the surface. These groups are formed by adsorption of atmospheric carbon dioxide on the strong basic surface sites O^{2-} and they are not totally eliminated by the thermal pre-treatment. Similarly to tin oxide, the immediate formation of both CO_2 and surface carbonates is observed when carbon monoxide is adsorbed in presence of oxygen (Fig. 3b). But, the surface carbonate species are quite intense and the complexity of the bands indicates that different types of surface basic sites are involved. Evacuation eliminates both carbon dioxide and carbonates but also causes a strong reduction of the sample, thus proving the easy and fast desorption of oxygen from the material (Fig. 3c).

The curve giving the variations of the transmitted infrared energy versus gas exposures clearly shows that, at 300 °C, the oxidation of indium oxide is rapidly completed under oxygen (Fig. 4a). Then, the response to CO is perfectly reproducible without any drift. It is worth noting that the formation of the large amount of several surface carbonate species, as

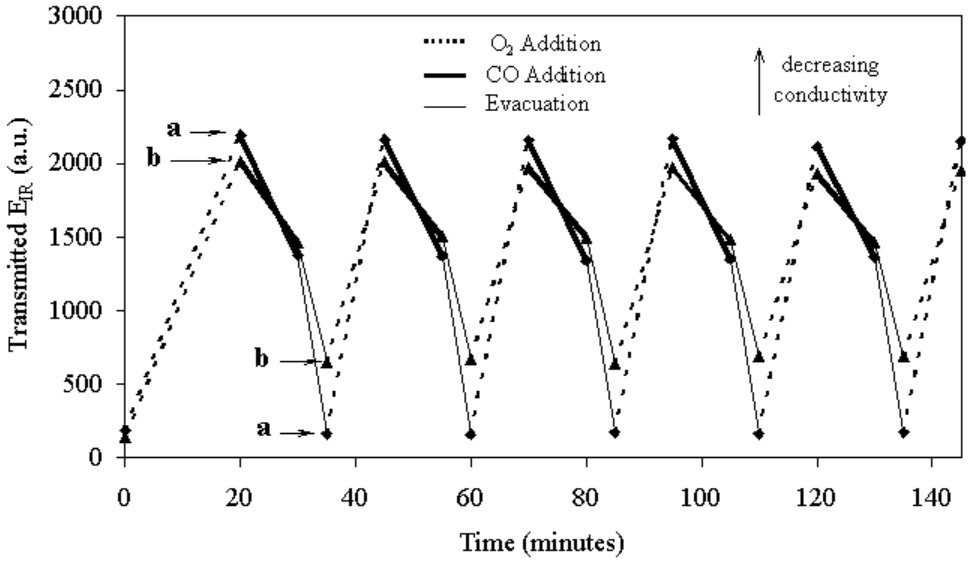

Fig. 4. Variations of the infrared energy (E_{IR}) transmitted by the In_2O_3 nanoparticles versus gas exposures: a) at 300 °C; b) at 150 °C.

observed in Fig. 3b, is not detrimental to the reversibility of the sensor response.

The same experiment performed at 150 °C (Fig. 4b) shows that, even at this moderate temperature, indium oxide is both strongly reduced by evacuation and rapidly oxidized under oxygen adsorption. This confirms that oxygen can easily diffuse into the In_2O_3 bulk. The reproducibility of the response toward CO is fair even though a slight drift is noted under oxygen. Unlike tin oxide at 150 °C, the formation of CO_2 and of various surface carbonate species is observed on the infrared spectra, although in lower amount than at 300 °C (not shown).

4.3. Tungsten oxide nanoparticles

The sensing properties of the tungsten oxide nanoparticles have been investigated under similar conditions. The infrared spectra clearly prove that CO_2 is formed when CO is adsorbed in presence of oxygen (Fig. 5a,b) although no carbonates are formed. It is also observed that the background

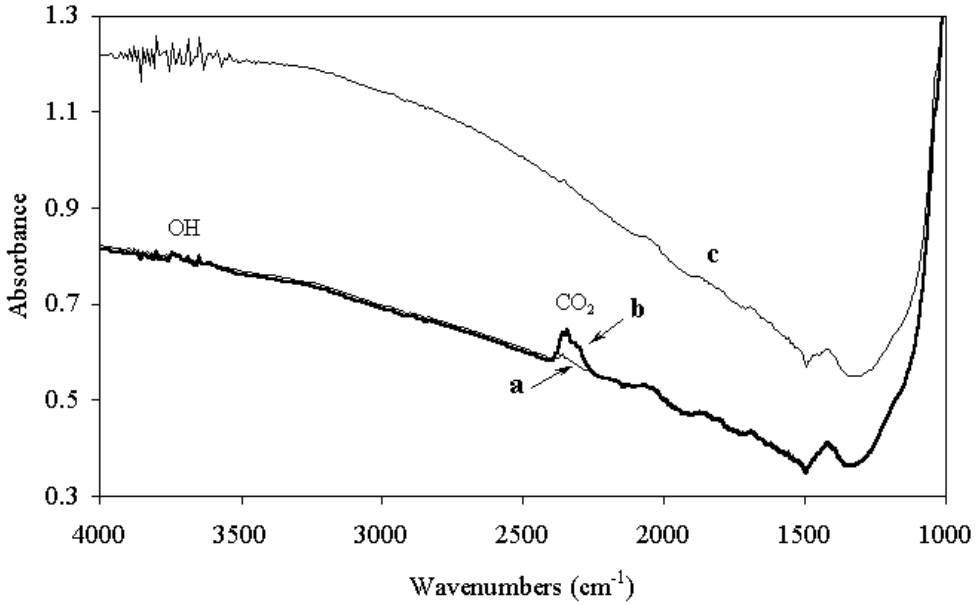

Fig. 5. Infrared transmission spectrum of the WO_3 nanoparticles at 300 °C: a) under 50 mbar oxygen; b) after adsorption of 10 mbar CO in presence of oxygen; c) after evacuation.

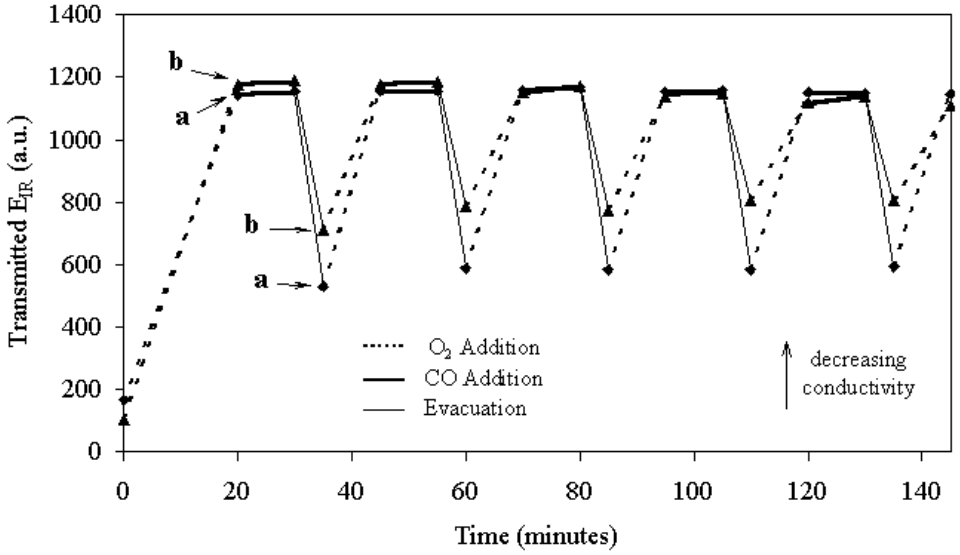

Fig. 6. Variations of the infrared energy (E_{IR}) transmitted by the WO_3 nanoparticles versus gas exposures: a) at 300 °C; b) at 150 °C.

infrared absorption is not modified by CO adsorption but is strongly increased by evacuation (Fig. 5c). Indeed, the variations of E_{IR} versus gas exposures surprisingly show that the response to CO at 300 °C is quasi nil and quite reproducible (Fig. 6a). The curve indicates that WO_3 is strongly reduced by evacuation but the adsorption of oxygen rapidly restores the original oxidation state which remains stable during the "CO addition-evacuation-oxygen addition" sequences.

At 150 °C, the sample oxidation under oxygen is fast and complete (Fig. 6b). When CO is adsorbed in presence of oxygen, a very weak but reproducible E_{IR} increase is observed, which means a slight decrease of the electrical conductivity. This result was not expected as the infrared spectra prove that a very small amount of CO_2 is formed (not shown). Like in the case of tin oxide and indium oxide nanoparticles, a slight drift of the oxidation level is observed.

4.4. Humidity effects on the sensing properties of the nanoparticles

A major drawback of the semiconductor gas sensors is their cross-sensitivity to humidity which makes their response unreliable for outdoor operation [8, 24, 25]. To evaluate the cross-sensitivity to humidity of these three nanosized powders, another series of experiments were performed consisting in the addition of two doses of CO, followed by the addition of three doses of CO mixed with water vapor (20% of water vapor in the mixture), referred to as "wet CO doses", followed by the addition of three new doses of dry CO. All doses were introduced in presence of oxygen. Besides, it is likely that the humidity effects will be stronger at lower temperatures and therefore, the testing temperature was set at 150 °C for all samples. The infrared spectra are not discussed here because the adsorption of the mixture of the three gases (oxygen, carbon monoxide and water vapor) on the nanoparticle surface makes the interpretation of the absorption bands rather complex and beyond the scope of this article. In the following, only the variations of the transmitted infrared energy versus gas exposures are analysed. These E_{IR} variations give a straightforward overview of the humidity effect on the sensing properties of the nanoparticles.

As a first example, it can be observed that, after addition of the first wet CO dose to the tin oxide nanoparticles, the original oxidation state is not restored under oxygen, and subsequently the responses to oxygen and CO are decreased (Fig. 7). In other words, after having been in contact with humidity, the tin oxide nanoparticles show a decrease of their sensitivity toward CO.

However, on indium oxide nanopowder, the amplitude of the response appears to be constant (Fig. 8). A drift of the signal under oxygen is noted due to the slower oxygen diffusion at 150 °C, as previously discussed. But this drift is not related to the presence of humidity as it is a steady process.

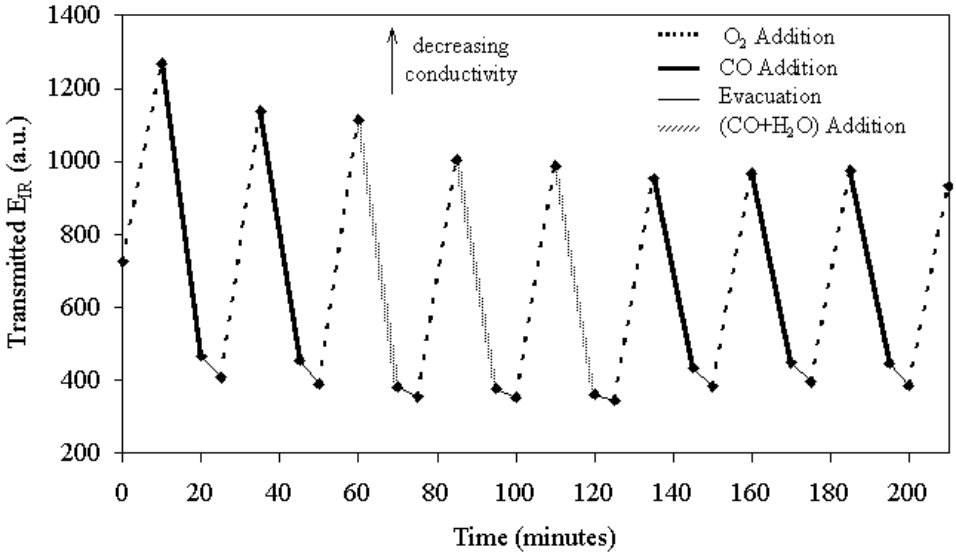

Fig. 7. Variations of the infrared energy (E_{IR}) transmitted by the SnO_2 nanoparticles versus gas exposures at 150 °C.

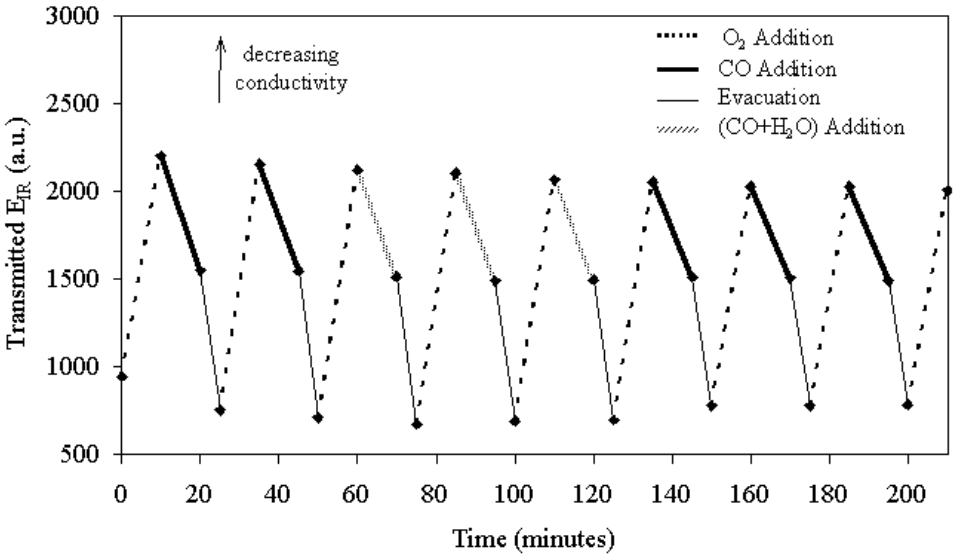

Fig. 8. Variations of the infrared energy (E_{IR}) transmitted by the In_2O_3 nanoparticles versus gas exposures at 150 °C.

As for tungsten oxide, the presence of humidity does not enhance the response toward CO which remains extremely weak compared to the response to oxygen (Fig. 9). The drift of the response to oxygen appears as explained in the previous section.

It is worth noting that, for the SnO_2 and In_2O_3 samples, the infrared spectra (not shown) indicate that the hydroxyl groups at the nanoparticle surface are involved in the surface reactions in presence of water vapor. These OH groups, whose concentration is particularly high at the SnO_2 surface, are reversibly modified in presence of humidity. Differently from tin oxide and indium oxide, the surface of tungsten oxide presents only an extremely small amount of hydroxyl groups (cf. Fig. 5). If we consider that the absence of surface hydroxyl groups might be related to the very low sensitivity of tungsten oxide to humidity, this would mean that a non-hydrophilic surface may be beneficial to the reduction of the cross-sensitivity to humidity.

5. CONCLUSIONS

FTIR spectroscopy has been used to screen the gas sensing properties of semiconducting nanoparticles before their integration in the fabrication process of gas sensors. The results obtained on the SnO_2, In_2O_3 and WO_3 nanoparticles can be summarized as follows:

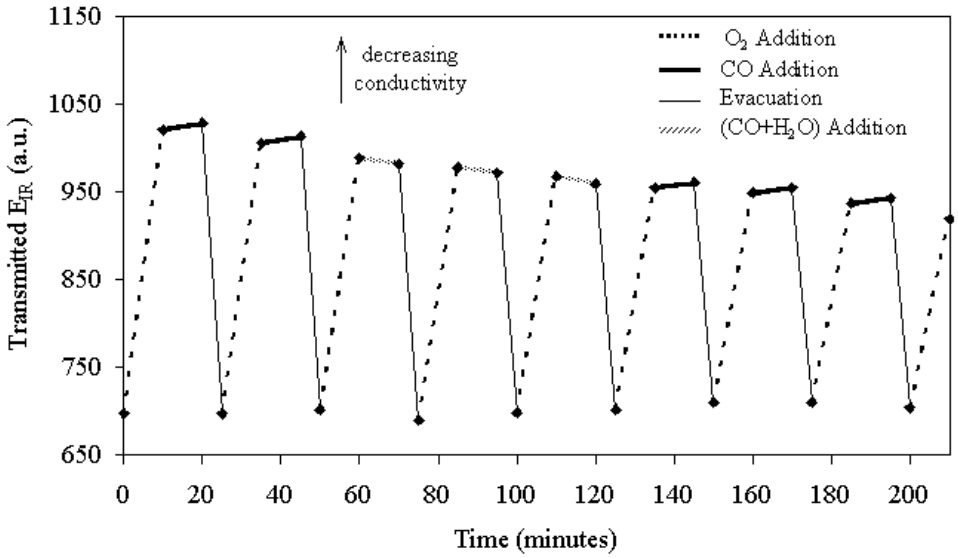

Fig. 9. Variations of the infrared energy (E_{IR}) transmitted by the WO_3 nanoparticles versus gas exposures at 150 °C.

- Tin oxide and indium oxide nanoparticles have a fairly good sensitivity toward CO but the sensitivity of indium oxide toward oxygen is higher;
- At 150 °C, indium oxide is less sensitive to humidity than tin oxide;
- Tungsten oxide shows a very weak sensitivity to CO and to humidity although the response toward oxygen is high;
- In general, a higher operating temperature leads to a faster response and a faster recovery of the oxidation state. However, in the case of indium oxide, the temperature has little influence on the response time. Indium oxide should be used preferably to tin oxide for CO detection at lower temperature.
- The high basicity of the indium oxide surface favoring the formation of carbonates does not imply a higher sensitivity to carbon monoxide compared to tin oxide, thus confirming that the carbonate formation is not a significant factor in the CO detection.

An important conclusion which can be drawn from these results is that the surface hydroxyl groups appear to play a major role in the cross-sensitivity to humidity. However, further experiments are needed to understand the complex reactions at the sensor surface in presence of humidity. It can already be envisaged to decrease the sensitivity to humidity by decreasing the density of the hydroxyl groups at the nanoparticle surface without jeopardizing the sensitivity to carbon monoxide and oxygen.

ACKNOWLEDGEMENTS

The authors acknowledge their partners of the European Consortium, and particularly Dr Hans Ferkel and his team at the University of Clausthal (Germany) for providing them with nanopowders, and Dr Gary Coles and his team at the University of Wales at Swansea (UK) for performing the electrical measurements on the real sensors.

This work has been financially supported by the Commission of the European Communities under the Information Society Technologies programme (contract number IST-12615).

REFERENCES

[1] *Directive 2000/69/CE of the European Parliament and of the Council of 16/11/2000*; *Directive 2001/81/CE of the European Parliament and of the Council of 23/10/2001;* http://europa.eu.int/eur-lex.

[2] G. Williams and G.S.V. Coles // *J. Mater. Chem.* **8** (1998) 1657.

[3] G. Williams and G.S.V. Coles // *MRS Bulletin* **24** (1999) 25.

[4] G. Williams and G.S.V. Coles, In: *SMOGLESS Final Report* (contract N: BRPR-CT95-0002), unpublished results (1999).

[5] M.-I. Baraton, In: *SMOGLESS Final Report* (contract N: BRPR-CT95-0002), unpublished results (1999).

[6] G.A. Somorjai // *MRS Bulletin* **23** (1998) 11.

[7] Y. Shimizu and M. Egashira // *MRS Bulletin* **24** (1999) 18.
[8] R.S. Morrison, In: *Semiconductors Sensors,* ed. by S.M. Sze (John Wiley & Sons, New York, 1994) p. 383.
[9] V.E. Henrich and P.A. Cox // *Applied Surf. Science* **72** (1993) 277.
[10] V.E. Henrich and P.A. Cox, *The Surface Science of Metal Oxides* (Cambridge University Press, Cambridge, 1994).
[11] P.K. Clifford, *Mechanisms of Gas Detection by Metal Oxide Surfaces, Ph.D. Thesis* (Carnegie Mellon Univ., Pittsburg, 1981).
[12] M.-I. Baraton, In: *Handbook of Nanostructured Materials and Nanotechnology,* ed. by H.S. Nalwa (Academic Press, San Diego, CA, 1999), p. 89.
[13] M.-I. Baraton and L. Merhari // *NanoStruct. Mater.* **10** (1998) 699.
[14] M.-I. Baraton, *In: NATO-ARW Series Nanostructured: Films and Coatings,* ed. by G.M. Chow *et al*. (Kluwer Academic Publishers, Dordrecht, 2000) p. 187.
[15] A.F. Gibson // *J. Scientific Instruments* **35** (1958) 273.
[16] N.J. Harrick // *Phys. Rev.* **125** (1962) 1165.
[17] N.J. Harrick, *Internal Reflection Spectroscopy* (Interscience, Wiley, New York, 1967).
[18] Y.J. Chabal // *Surf. Science Reports* **8** (1988) 211.
[19] M.-I. Baraton and L. Merhari // *Mater. Transactions* **42** (2001) 1616.
[20] G. Herzberg, *Molecular Spectra and Molecular Structure – II. Infrared and Raman Spectra of Polyatomic Molecules, 10th printing* (D. Van Nostrand Company Inc., Princeton, 1962).
[21] P.G. Harrison and M.J. Willett // *Nature* **332** (1988) 337.
[22] M.J. Willett, In: *Techniques and Mechanisms in Gas Sensing*, ed. by P.T. Mosley, J.W.O. Norris and D.E. Williams (Adams Hilger, Bristol, 1991) p. 61.
[23] G. Busca and V. Lorenzelli // *Mater. Chem.* **7** (1982) 89.
[24] N. Barsan, M. Schweizer-Berberich and W. Göpel, Fresenius // *J. Anal. Chem.* **365** (1999) 287.
[25] K.R. Han, C.S. Kim, K.T. Kang, H.J. Koo, D.I. Kang and H. Jingwen // *Sensors Actuat. B* **81** (2002) 182.